Spectra of sparse random matrices

2008 J. Phys. A: Math. Theor. 41 295002

(http://iopscience.iop.org/1751-8121/41/29/295002)

IOP PUBLISHING JOURNAL OF PHYSICS A: MATHEMATICAL AND THEORETICAL

J. Phys. A: Math. Theor. **41** (2008) 295002 (21pp) doi:10.1088/1751-8113/41/29/295002

Spectra of sparse random matrices

Reimer Kühn

Mathematics Department, King's College London, Strand, London WC2R 2LS, UK

Received 26 March 2008, in final form 7 May 2008
Published 26 June 2008
Online at stacks.iop.org/JPhysA/41/295002

Abstract

We compute the spectral density for ensembles of sparse symmetric random matrices using replica. Our formulation of the replica-symmetric ansatz shares the symmetries of that suggested in a seminal paper by Rodgers and Bray (symmetry with respect to permutation of replica *and* rotation symmetry in the space of replica), but uses a different representation in terms of superpositions of Gaussians. It gives rise to a pair of integral equations which can be solved by a stochastic population-dynamics algorithm. Remarkably our representation allows us to identify pure-point contributions to the spectral density related to the existence of normalizable eigenstates. Our approach is not restricted to matrices defined on graphs with Poissonian degree distribution. Matrices defined on regular random graphs or on scale-free graphs, are easily handled. We also look at matrices with row constraints such as discrete graph Laplacians. Our approach naturally allows us to unfold the total density of states into contributions coming from vertices of different local coordinations and an example of such an unfolding is presented. Our results are well corroborated by numerical diagonalization studies of large finite random matrices.

PACS numbers: 02.50.−r, 05.10.−a

1. Introduction

Since its inception by Wigner in the context of describing spectra of excited nuclei [1], random matrix theory (RMT) has found applications in numerous areas of science, including questions concerning the stability of complex systems [2], electron localization [3], quantum chaos [4], quantum chromo dynamics [5], finance [6, 7], the physics of glasses both at elevated [8, 9] and low [10, 11] temperatures, number theory [12] and many more. For an extensive review describing many of the applications in physics see, e.g. [13].

In the present paper, we revisit the problem of determining the spectral density for ensembles of sparse random matrices pioneered two decades ago in seminal papers by Bray and Rodgers [14, 15]. The problem has in recent years received much renewed interest in connection with the study of complex networks, motivated, for instance, by the fact that geometric and topological properties of networks are reflected in spectral properties of

adjacency matrices defining the networks in question [16, 17]. Also, phenomena such as non-exponential relaxation in glassy systems and gels [15, 18]—intimately related to Lifshitz tails [19] and Griffiths' singularities in disordered systems [20]—as well as Anderson localization of electronic [21] or vibrational [22] states have been studied in sparsely connected random systems, as finite-dimensional versions of these problems have proven to be extremely difficult to analyse.

A wealth of analytical and numerical results has been accumulated on these systems in recent years. In particular, the Rodgers–Bray integral equation [14], whose solution allows us to express the spectral density, was also obtained using a supersymmetry approach [23], and it was recently derived rigorously by Khorunzhy *et al* [24], thereby establishing the symmetry assumptions required in the solutions of [14, 23] as justified.

Progress has, however, been partly hampered by the fact that full solutions of the Rodgers–Bray integral equation [14] have so far eluded us, and asymptotic analyses and other approximations had to come in for help. For example expansions for large average connectivities c [14] have revealed that Wigner's semicircle law [25] is recovered in the limit $c \to \infty$, and exponential tails in the spectral density extending beyond the edge of the Wigner semicircle were shown to exist at finite c by means of a (nonperturbative) saddle-point analysis. Away from the large c limit, other approximation schemes such as the single defect approximation (SDA) and the effective medium approximation (EMA) [17, 26, 27] (see [28] for a very recent application), as well as numerical diagonalization (e.g. [29]). have frequently been used to analyse spectral properties of large random matrices.

In what follows we describe some significant progress in the understanding of this problem, based upon advances in the statistical mechanical analysis of sparsely connected spin-glass like systems seen in the last couple of years [30, 31]—in the present context in particular the proposal of a stochastic population-dynamics algorithm [31] to solve the nonlinear integral equations appearing in the solution of these problems, and the recent generalization of these methods to systems with continuous degrees of freedom, such as models of sparsely connected vector spins [32], or finitely coordinated models for low-temperature phases of amorphous systems [33].

It is well known that the average spectral density $\overline{\rho}_N(\lambda)$ (the average density of eigenvalues λ) of an ensemble $\mathcal{M}$ of $N \times N$ matrices M can be computed from the ensemble average of the imaginary part of their resolvent via

$$\overline{\rho}_N(\lambda) = \frac{1}{\pi N} \operatorname{Im} \operatorname{Tr} \overline{[\lambda_\varepsilon \mathbb{1} - M]^{-1}}. \tag{1}$$

Here $\mathbb{1}$ is the $N \times N$ unit matrix, and $\lambda_\varepsilon = \lambda - \mathrm{i}\varepsilon$, the limit $\varepsilon \to 0^+$ being understood. Following Edwards and Jones [34], one can express this result in terms of the Gaussian integral

$$Z_N = \int \prod_{i=1}^{N} \frac{\mathrm{d}u_i}{\sqrt{2\pi/\mathrm{i}}} \exp\left\{ -\frac{\mathrm{i}}{2} \sum_{i,j} u_i (\lambda_\varepsilon \delta_{ij} - M_{ij}) u_j \right\} \tag{2}$$

as

$$\overline{\rho}_N(\lambda) = -\frac{2}{\pi N} \operatorname{Im} \frac{\partial}{\partial \lambda} \overline{\ln Z_N} = \frac{1}{N} \operatorname{Re} \sum_{i=1}^{N} \overline{\langle u_i^2 \rangle}, \tag{3}$$

using the replica method to evaluate the average of the logarithm in (3) over the ensemble $\mathcal{M}$ of matrices M under consideration. The 'averages' $\langle u_i^2 \rangle$ in (3) are evaluated with respect to the

'Gaussian measure' defined by (2).[1] This has been the path taken in [14]; we shall initially follow their reasoning.

Disregarding the complex nature of the 'Hamiltonian' in the evaluation of (2), the mathematical problem posed in (2), (3) is analogous to the evaluation of an 'internal energy' of a disordered system with quenched disorder. Within the general class of finitely coordinated amorphous model systems considered in [33], that represented by (2), (3) constitutes a particular subclass, namely that of harmonically coupled systems, for which the analysis was found to be *much* simpler than for systems involving anharmonic couplings. Indeed, while the solution of the latter required the self-consistent determination of probability distributions over infinite-dimensional function-spaces, it was realized in [33] that solutions of harmonically coupled systems could be formulated in terms of superpositions of Gaussians, and that the self-consistency problem reduced to the (much simpler) problem of a self-consistent determination of the probability distribution of their variances.

It can be fairly argued that this last insight is, in fact, easier to obtain within a Bethe-Peierls or cavity-type approach [31], in which (2) is recursively evaluated *for given instances* on graphs which are locally tree-like, ignoring correlations among subtrees—an approximation that becomes exact, e.g., for random graphs that remain finitely coordinated in the thermodynamic limit. This approach is taken in a separate publication [35], in which (finite) single-instances and promising algorithmic aspects of the problem are being highlighted.

Although [33] describes all technical details needed for a replica analysis of the present problem, we shall nevertheless reproduce the key steps here, both to keep the paper self-contained, and to point out along the way where the point of departure between our approach and that of [14] occurs.

The remainder of the paper is organized as follows. In section 2, we describe the replica analysis of the problem posed by (2), (3), specializing to matrices defined on Poissonian (Erdös–Renyi) random graphs. It has been known for some time [14, 34] that the replica-symmetric high-temperature solution—i.e., a solution preserving both, permutation-symmetry among replica, and rotational symmetry in the space of replica—is exact for problems of the type considered here. Accordingly, a representation that respects these symmetries is formulated in section 2.1. It is at this point where our formulation departs from that of [14]. In section 3 we present results for a variety of examples, and compare with numerical diagonalization results for large finite matrices to assess their quality. In sufficiently sparse graphs, one expects localized states, i.e. eigenvalues in the point spectrum with normalizable eigenvectors to exist. It is one of the remarkable and surprising results of the present study that our formulation allows us to identify the contribution of the point spectrum to the overall spectral density. The signatures of localization within our approach are discussed throughout section 3, with inverse participation ratios (IPRs) as a tool supporting our conjecture briefly looked at in section 3.2. A more detailed and quantitative investigation of localization—primarily for (discrete) Schrödinger operators on sparse random graphs—will be reserved to a separate publication [36]. Matrices with bimodal instead of Gaussian random couplings are studied in section 3.3. As the formal structure of the self-consistency problem remains unaltered when the Poissonian random graphs are replaced by graphs with other degree distributions [33], we can exploit this fact to present results for regular and scale-free random graphs in section 3.4. Modifications needed to treat matrices with row constraints, such as discrete graph Laplacians are outlined in section 3.5. Our approach naturally allows us to unfold the total density of states into contributions coming from vertices of different

[1] Note that we are using probabilistic notions in a loose, metaphorical sense, as the Gaussian measures used in these calculations are complex.

local coordinations, and we finally present an example of such an unfolding in section 3.6. Section 4 contains a brief summary and an outlook on promising directions for future research.

2. Replica analysis

2.1. General formulation

Here we briefly outline the evaluation of (2), (3) for sparse symmetric matrices M of the form

$$M_{ij} = c_{ij} K_{ij}, \tag{4}$$

in which $C = \{c_{ij}\}$ is a symmetric adjacency matrix of an undirected random graph (with $c_{ii} = 0$), and the non-zero elements of M are specified by the K_{ij}, also taken to be symmetric in the indices. Within the present outline we restrict ourselves for the sake of simplicity to adjacency matrices of Erdös–Renyi random graphs, with

$$P(\{c_{ij}\}) = \prod_{i<j} p(c_{ij})\delta_{c_{ij},c_{ji}} \qquad \text{and} \qquad p(c_{ij}) = \left(1 - \frac{c}{N}\right)\delta_{c_{ij},0} + \frac{c}{N}\delta_{c_{ij},1},$$

exhibiting a Poissonian degree distribution with average coordination c. We note at the outset that formal results carry over without modification to other cases [33]. There is no need at this point to specify the distribution of the K_{ij}, but we shall typically look at Gaussian and bimodal distributions.

The average (3) is evaluated using replica $\overline{\ln Z_N} = \lim_{n\to 0} \frac{1}{n} \ln \overline{Z_N^n}$, starting with integer numbers of replica as usual. After performing the average over the distribution of the connectivities c_{ij} one obtains

$$\overline{Z_N^n} = \int \prod_{ia} \frac{\mathrm{d}u_{ia}}{\sqrt{2\pi/\mathrm{i}}} \exp\left\{-\frac{\mathrm{i}}{2}\lambda_\varepsilon \sum_{i,a} u_{ia}^2 + \frac{c}{2N}\sum_{ij}\left(\left\langle \exp\left(\mathrm{i}K\sum_a u_{ia}u_{ja}\right)\right\rangle_K - 1\right)\right\}, \tag{5}$$

in which $a = 1, \ldots, n$ labels the replica, and $\langle\cdots\rangle_K$ refers to an average over the distribution of the K_{ij}. The double sum appearing in the exponential of (5) can be expressed in terms of integrals over the replicated density

$$\rho(\boldsymbol{u}) = \frac{1}{N}\sum_i \prod_a \delta(u_a - u_{ia}), \qquad \text{with} \quad \boldsymbol{u} \equiv (u_1, u_2, \ldots, u_n), \tag{6}$$

as

$$\frac{c}{2N}\sum_{ij}\left(\left\langle \exp\left(\mathrm{i}K\sum_a u_{ia}u_{ja}\right)\right\rangle_K - 1\right)$$
$$= N\frac{c}{2}\int \mathrm{d}\boldsymbol{u}\,\rho(\boldsymbol{u})\,\mathrm{d}\boldsymbol{v}\,\rho(\boldsymbol{v})\left(\left\langle \exp\left(\mathrm{i}K\sum_a u_a v_a\right)\right\rangle_K - 1\right).$$

A decoupling of sites is achieved by enforcing the definition of ρ via functional δ distributions,

$$1 = \int \mathcal{D}\rho\,\mathcal{D}\hat{\rho}\exp\left\{-\mathrm{i}\int \mathrm{d}\boldsymbol{u}\,\hat{\rho}(\boldsymbol{u})\left(N\rho(\boldsymbol{u}) - \sum_i\prod_a \delta(u_a - u_{ia})\right)\right\}. \tag{7}$$

This gives (using shorthands of the form $\mathrm{d}\rho(\boldsymbol{u}) \equiv \mathrm{d}\boldsymbol{u}\rho(\boldsymbol{u})$ where useful)

$$\overline{Z_N^n} = \int \mathcal{D}\rho \int \mathcal{D}\hat{\rho} \exp\left\{ N \left[\frac{c}{2} \int \mathrm{d}\rho(\boldsymbol{u})\, \mathrm{d}\rho(\boldsymbol{v}) \left(\left\langle \exp\left(\mathrm{i}K \sum_a u_a v_a \right) \right\rangle_K - 1 \right) \right.\right.$$
$$\left.\left. - \int \mathrm{d}\boldsymbol{u}\, \mathrm{i}\hat{\rho}(\boldsymbol{u})\rho(\boldsymbol{u}) + \ln \int \prod_a \frac{\mathrm{d}u_a}{\sqrt{2\pi/\mathrm{i}}} \exp\left(\mathrm{i}\hat{\rho}(\boldsymbol{u}) - \frac{\mathrm{i}}{2}\lambda_\varepsilon \sum_a u_a^2 \right) \right] \right\}, \tag{8}$$

allowing us to evaluate $N^{-1} \ln \overline{Z_N^n}$ by a saddle-point method. The stationarity conditions w.r.t. variations of ρ and $\hat{\rho}$ read as

$$\mathrm{i}\hat{\rho}(\boldsymbol{u}) = c \int \mathrm{d}\rho(\boldsymbol{v}) \left(\left\langle \exp\left(\mathrm{i}K \sum_a u_a v_a \right) \right\rangle_K - 1 \right), \tag{9}$$

$$\rho(\boldsymbol{u}) = \frac{\exp\left(\mathrm{i}\hat{\rho}(\boldsymbol{u}) - \frac{\mathrm{i}}{2}\lambda_\varepsilon \sum_a u_a^2 \right)}{\int \mathrm{d}\boldsymbol{u} \exp\left(\mathrm{i}\hat{\rho}(\boldsymbol{u}) - \frac{\mathrm{i}}{2}\lambda_\varepsilon \sum_a u_a^2 \right)}. \tag{10}$$

The way in which sites are decoupled constitutes the first point of departure between our treatment and that of [14] and subsequent analyses inspired by it (e.g. [37, 38]). In these papers the averaged exponential expressions in the exponent of (5),

$$f(\boldsymbol{u}_i \cdot \boldsymbol{v}_j) = f\left(\sum_a u_{ia} v_{ja} \right) = \left\langle \exp\left(\mathrm{i}K \sum_a u_{ia} v_{ja} \right) \right\rangle_K - 1, \tag{11}$$

is expanded, and an infinite family of multi-replica generalizations of Edwards Anderson order parameters (and corresponding Hubbard–Stratonovich transformations) are used to decouple the sites, much as in the treatment of the dilute spin-glass problem by Viana and Bray [39]. The authors then use the expansion and the infinite set of self-consistency equations for the multi-replica generalizations of Edwards Anderson order parameters to construct an equivalent *functional* self-consistency problem described by a nonlinear integral equation for a function g defined via a suitable 'average' of f; see [14] for details. Our treatment in this respect is closer in spirit to the alternative approach of Kanter and Sompolinsky [40] who treat local field distributions (which in the general context of disordered amorphous systems discussed in [33] become distributions of local potentials) as the primary object of their theory.

However, the difference between our treatment and that of [14] is at this point still superficial. Indeed, we can combine (9) and (10) to give

$$\mathrm{i}\hat{\rho}(\boldsymbol{u}) = \frac{\int \mathrm{d}\boldsymbol{v}\, f(\boldsymbol{u} \cdot \boldsymbol{v}) \exp\left(\mathrm{i}\hat{\rho}(\boldsymbol{v}) - \frac{\mathrm{i}}{2}\lambda_\varepsilon \boldsymbol{v}^2 \right)}{\int \mathrm{d}\boldsymbol{v} \exp\left(\mathrm{i}\hat{\rho}(\boldsymbol{v}) - \frac{\mathrm{i}}{2}\lambda_\varepsilon \boldsymbol{v}^2 \right)}, \tag{12}$$

which is the Rodgers–Bray integral equation for general distributions of non-zero bond strengths (before exploiting replica symmetry and taking the $n \to 0$-limit), if we identify our 'conjugate density' $\hat{\rho}$ with the function g introduced by Rodgers and Bray [14] via

$$\mathrm{i}\hat{\rho}(\boldsymbol{u}) = cg(\boldsymbol{u}). \tag{13}$$

2.2. *Replica symmetry*

To deal with the $n \to 0$ limit in these equations, assumptions concerning the invariance properties of the solutions $\rho(\boldsymbol{u})$ and $\hat{\rho}(\boldsymbol{u})$ of (9) and (10)—alternatively of the solution $\mathrm{i}\hat{\rho}(\boldsymbol{u}) = cg(\boldsymbol{u})$ of (12)—under transformations among the replica are required. It has been established for some time [14, 34] that the replica-symmetric high-temperature solution—i.e.,

a solution preserving both, permutation-symmetry among replica, and rotational symmetry in the space of replica—is exact for problems of the type considered here. The work of Khorunzhy *et al* [24] implies that this assumption is rigorously justified.

It is here where the paths taken in the present paper and in [14] really bifurcate. In [14], the assumption $g(\boldsymbol{u}) = g(u)$, with $u = |\boldsymbol{u}|$ is used to perform the angular integrals in n-dimensional polar coordinates in (12), resulting in an integral equation for $g(u)$ in the $n \to 0$-limit. This integral equation has, however, so far resisted exhaustive analysis or full numerical solution.

In the present paper we follow [33], using a replica-symmetric *ansatz* in which ρ and $\hat{\rho}$ are represented as *uncountably infinite* superpositions of normalized (though complex!) Gaussians of the form

$$\rho(\boldsymbol{u}) = \int \mathrm{d}\omega\, \pi(\omega) \prod_a \frac{\exp\left[-\frac{\omega}{2}u_a^2\right]}{Z(\omega)}, \tag{14}$$

$$\mathrm{i}\hat{\rho}(\boldsymbol{u}) = \hat{c} \int \mathrm{d}\hat{\omega}\, \hat{\pi}(\hat{\omega}) \prod_a \frac{\exp\left[-\frac{\hat{\omega}}{2}u_a^2\right]}{Z(\hat{\omega})}, \tag{15}$$

utilizing the observation made in [33] that such superpositions of Gaussians would provide exact solutions for harmonically coupled amorphous systems. An analogous observation has, in fact, been made earlier in the context of solving models of randomly and permanently cross-linked polymers [41].

The integrals in (14) and (15) extend over the complex half-planes $\mathrm{Re}\,\omega \geqslant 0$ and $\mathrm{Re}\,\hat{\omega} \geqslant 0$, respectively. The weight functions π and $\hat{\pi}$ have to be determined self-consistently. We take them to be normalized, $\int \mathrm{d}\omega\, \pi(\omega) = 1$, and similarly for $\hat{\pi}$, requiring that the constant $\hat{c}$ in (15) be properly chosen. We note that our ansatz exhibits permutation symmetry among replica as well as rotational symmetry in the space of replica.

Below we show that this ansatz does indeed provide a *self-consistent* solution of the fixed-point equations characterizing the dominant contribution to (8). Provided that there are no other, coexisting solutions to the problem (which would seem implausible in view of the Gaussian nature of the original problem), this would solve our problem. As a further justification one might note that (6) would be expressible in terms of a superposition of (single-site) marginals. For every *instance* of a replicated version of the Gaussian integral (2), these would indeed be superpositions of Gaussians. Lastly, we note expansions (14) and (15) are expansion in terms of *over-complete* families of functions on $L^2(\mathbb{R})$. To see this consider (14). Replica symmetry and rotational invariance of the integral representation in the space of replica entails that we can write $\rho(\boldsymbol{u}) = \rho(x)$ with $x \equiv \frac{1}{2}u^2$; this allows us to reformulate (14) as

$$\rho(x) = \int \mathrm{d}\omega\, \pi_n(\omega) \exp(-\omega x) \tag{16}$$

with $\pi_n(\omega) \equiv \pi(\omega)/Z(\omega)^n$, showing that the integral representations contain Fourier transforms as a special subclass (in which the integral is restricted to the region $\mathrm{Re}(\omega) = 0$). An analogous argument holds for $\mathrm{i}\hat{\rho}(\boldsymbol{u})$. A proper solution to the problem, as opposed to an approximation will then be obtainable, if the family of functions is sufficiently rich to represent the solution of the Rodgers–Bray integral equations. Our results below strongly indicate that this is indeed the case, though a rigorous proof is missing, and would of course be desirable.

Expressing (8) in terms of π and $\hat{\pi}$, we get

$$\overline{Z_N^n} = \int \mathcal{D}\pi\, \mathcal{D}\hat{\pi}\, \exp\{N[G_1[\pi] + G_2[\hat{\pi}, \pi] + G_3[\hat{\pi}]]\}. \tag{17}$$

As $n \to 0$, the functionals G_1, G_2 and G_3 evaluate to

$$G_1[\pi] \simeq n\frac{c}{2}\int \mathrm{d}\pi(\omega)\,\mathrm{d}\pi(\omega')\left\langle \ln \frac{Z_2(\omega,\omega',K)}{Z(\omega)Z(\omega')}\right\rangle_K, \tag{18}$$

$$G_2[\hat\pi,\pi] \simeq -\hat c - n\hat c\int \mathrm{d}\hat\pi(\hat\omega)\,\mathrm{d}\pi(\omega)\ln\frac{Z(\hat\omega+\omega)}{Z(\hat\omega)Z(\omega)}, \tag{19}$$

$$G_3[\hat\pi] \simeq \hat c + n\sum_{k=0}^{\infty} p_{\hat c}(k)\int \{\mathrm{d}\hat\pi\}_k \ln\frac{Z_{\lambda_\varepsilon}(\{\hat\omega\}_k)}{\prod_{\ell=1}^k Z(\hat\omega_\ell)}, \tag{20}$$

in which we have introduced the shorthands $\mathrm{d}\pi(\omega) \equiv \mathrm{d}\omega\,\pi(\omega)$ and similarly for $\hat\pi$, as well as $\{\mathrm{d}\hat\pi\}_k \equiv \prod_{\ell=1}^k \mathrm{d}\hat\pi(\hat\omega_\ell)$, and $\{\hat\omega\}_k = \sum_{\ell=1}^k \hat\omega_\ell$, a Poissonian connectivity distribution

$$p_{\hat c}(k) = \frac{\hat c^k}{k!}\exp[-\hat c] \tag{21}$$

with average connectivity $\langle k\rangle = \hat c$, and the 'partition functions'

$$Z(\omega) = \int \mathrm{d}u \exp\left[-\frac{\omega}{2}u^2\right] = \sqrt{2\pi/\omega}, \tag{22}$$

$$Z_{\lambda_\varepsilon}(\{\hat\omega\}_k) = \int \frac{\mathrm{d}u}{\sqrt{2\pi/\mathrm{i}}}\exp\left[-\frac{1}{2}(\mathrm{i}\lambda_\varepsilon + \{\hat\omega\}_k)u^2\right] = \left(\frac{\mathrm{i}}{\mathrm{i}\lambda_\varepsilon + \{\hat\omega\}_k}\right)^{1/2}, \tag{23}$$

$$Z_2(\omega,\omega',K) = \int \mathrm{d}u\,\mathrm{d}v \exp\left[-\frac{1}{2}(\omega u^2 + \omega' v^2 - 2\mathrm{i}Kuv)\right] = \frac{2\pi}{\sqrt{\omega\omega' + K^2}}. \tag{24}$$

Note that the $\mathcal{O}(1)$ contributions of G_2 and G_3 in the exponent of (8) cancel in their sum.

The stationarity condition of the functional integral (8) w.r.t. variations of ρ and $\hat\rho$ is reformulated in terms of stationarity conditions w.r.t. variations π and $\hat\pi$,

$$\hat c\int \mathrm{d}\hat\pi(\hat\omega)\ln\frac{Z(\hat\omega+\omega)}{Z(\hat\omega)Z(\omega)} = c\int \mathrm{d}\pi(\omega')\left\langle \ln\frac{Z_2(\omega,\omega',K)}{Z(\omega)Z(\omega')}\right\rangle_K + \mu, \tag{25}$$

$$\hat c\int \mathrm{d}\pi(\omega)\ln\frac{Z(\hat\omega+\omega)}{Z(\hat\omega)Z(\omega)} = \sum_{k\geqslant 1} k p_{\hat c}(k)\int \{\mathrm{d}\hat\pi\}_{k-1}\ln\frac{Z_{\lambda_\varepsilon}(\hat\omega+\{\hat\omega\}_{k-1})}{Z(\hat\omega)\prod_{\ell=1}^{k-1}Z(\hat\omega_\ell)} + \hat\mu, \tag{26}$$

with μ and $\hat\mu$ being Lagrange multipliers to take the normalization of π and $\hat\pi$ into account.

The conditions that (25) must hold for all ω and similarly that (26) must hold for all $\hat\omega$ can be translated [31] into

$$\hat\pi(\hat\omega) = \frac{c}{\hat c}\int \mathrm{d}\pi(\omega')\langle\delta(\hat\omega - \hat\Omega(\omega',K))\rangle_K, \tag{27}$$

$$\pi(\omega) = \sum_{k\geqslant 1}\frac{k}{\hat c}p_{\hat c}(k)\int\{\mathrm{d}\hat\pi\}_{k-1}\delta\left(\omega - \Omega(\{\hat\omega\}_{k-1})\right), \tag{28}$$

in which $\hat\Omega(\omega',K)$ and $\Omega(\{\hat\omega\}_{k-1})$ are defined via

$$Z(\omega+\hat\Omega(\omega',K)) = \frac{Z_2(\omega,\omega',K)}{Z(\omega')} \quad\Leftrightarrow\quad \hat\Omega(\omega',K) = \frac{K^2}{\omega'}, \tag{29}$$

and

$$\Omega(\{\hat{\omega}\}_{k-1}) = \mathrm{i}\lambda_\varepsilon + \sum_{\ell=1}^{k-1} \hat{\omega}_\ell, \tag{30}$$

respectively. Given that π is normalized, it follows from (27) that the same is true for $\hat{\pi}$, provided $\hat{c} = c$, so the fixed point equations take their final form as

$$\hat{\pi}(\hat{\omega}) = \int \mathrm{d}\pi(\omega') \langle \delta(\hat{\omega} - \hat{\Omega}(\omega', K)) \rangle_K, \tag{31}$$

$$\pi(\omega) = \sum_{k \geqslant 1} \frac{k}{c} p_c(k) \int \{\mathrm{d}\hat{\pi}\}_{k-1} \delta\left(\omega - \Omega(\{\hat{\omega}\}_{k-1})\right). \tag{32}$$

These equations can be seen as special cases of the general framework derived in [33], when restricted to harmonically coupled random systems. In [33] it is shown that they hold—unmodified—for non-Poissonian degree distributions as well, as long as the average connectivity in these systems remains finite.

Note that π and $\hat{\pi}$—self-consistently—have support in $\mathrm{Re}\,\omega \geqslant 0$ and $\mathrm{Re}\,\hat{\omega} \geqslant 0$ as required. The equations take a form that suggests solving them via a stochastic population-based algorithm, as described in the appendix.

To obtain the thermodynamic limit of the spectral density we have to evaluate the λ derivative (3). We note that this requires to consider only the *explicit* λ dependence in (17), as the rhs is evaluated where the exponent is stationary w.r.t. variations of π and $\hat{\pi}$. Thus only the λ derivative of G_3 in (20) is involved, giving

$$\begin{aligned} \overline{\rho}(\lambda) &= \frac{1}{\pi} \mathrm{Im} \sum_{k=0}^{\infty} p_c(k) \int \{\mathrm{d}\hat{\pi}\}_k \frac{\mathrm{i}}{\mathrm{i}\lambda_\varepsilon + \{\hat{\omega}\}_k} \\ &= \frac{1}{\pi} \sum_{k=0}^{\infty} p_c(k) \int \{\mathrm{d}\hat{\pi}\}_k \frac{\mathrm{Re}(\{\hat{\omega}\}_k + \varepsilon)}{(\mathrm{Re}(\{\hat{\omega}\}_k + \varepsilon))^2 + (\lambda + \mathrm{Im}\{\hat{\omega}\}_k)^2}. \end{aligned} \tag{33}$$

This expression has a natural interpretation as a sum of contributions of local densities of state of sites with connectivities k, weighted according to their probability of occurrence. Referring to (3), we may further identify the

$$\sigma_k^2 = \frac{1}{\pi} \mathrm{Im} \frac{\mathrm{i}}{\mathrm{i}\lambda_\varepsilon + \{\hat{\omega}\}_k} \tag{34}$$

as realizations of the variance of (Gaussian) marginals on sites of coordination k.

In order to allow a proper interpretation and a succinct discussion of the results obtained by evaluating (33) via sampling from a population, and with an eye towards disentangling singular (pure point) and continuous contributions to the spectral density, we find it useful to introduce the density

$$P(a, b) = \sum_k p_c(k) \int \{\mathrm{d}\hat{\pi}\}_k \delta\left(a - \mathrm{Re}\{\hat{\omega}\}_k\right) \delta\left(b - \mathrm{Im}\{\hat{\omega}\}_k\right), \tag{35}$$

with $a \geqslant 0$ by construction. The density of states can then be expressed as an integral over P,

$$\overline{\rho}(\lambda) = \int \frac{\mathrm{d}a\,\mathrm{d}b}{\pi} P(a, b) \frac{a + \varepsilon}{(a + \varepsilon)^2 + (b + \lambda)^2}. \tag{36}$$

Noting the singular nature of the above integrand in the limit $\varepsilon \to 0$ for $a = 0$, we propose to isolate possible singular contributions to the spectral density by writing

$$P(a, b) = P_0(b)\delta(a) + \tilde{P}(a, b). \tag{37}$$

This gives

$$\overline{\rho}(\lambda) = \int \mathrm{d}b\, P_0(b)\mathcal{L}_\varepsilon(b+\lambda) + \int_{a>0} \frac{\mathrm{d}a\,\mathrm{d}b}{\pi}\tilde{P}(a,b)\frac{a+\varepsilon}{(a+\varepsilon)^2+(b+\lambda)^2}, \quad (38)$$

in which $\mathcal{L}_\varepsilon$ denotes a Lorentzian of width ε. Our results below *strongly suggest* that, when the limit $\varepsilon \to 0$ is taken—thereby $\mathcal{L}_\varepsilon(x) \to \delta(x)$—a non-zero value of

$$P_0(-\lambda) = \lim_{\varepsilon\to 0}\int \mathrm{d}b\, P_0(b)\mathcal{L}_\varepsilon(b+\lambda) \quad (39)$$

gives the contribution of the point spectrum to the overall spectral density, which is associated with normalizable (hence localized) states.

This concludes the general framework.

3. Results

In what follows, we report results for a variety of different ensembles of sparse random matrices, in order to explore the capabilities and limitations of our approach. In order to properly appreciate the results presented below, it is worth pointing out that within our stochastic population-dynamics based approach to solving the fixed point equations (31) and (32), the integrals (33), or (36), (38) are evaluated by *sampling* from a population. Denoting by $\mathcal{N}$ the number of samples (a_i, b_i) taken, we have, e.g.,

$$\overline{\rho}(\lambda) \simeq \frac{1}{\mathcal{N}}\left[\sum_{\substack{i=1\\a_i=0}}^{\mathcal{N}} \mathcal{L}_\varepsilon(b_i+\lambda) + \frac{1}{\pi}\sum_{\substack{i=1\\a_i>0}}^{\mathcal{N}} \frac{a_i+\varepsilon}{(a_i+\varepsilon)^2+(b_i+\lambda)^2}\right] \quad (40)$$

as an approximation of (38). The $\varepsilon \to 0$-limit is clearly singular in the first contribution to (40). If $b_i + \lambda \neq 0$ for all b_i in the sample, one obtains zero in the $\varepsilon \to 0$-limit, whereas one obtains a diverging contribution, if $b_i + \lambda = 0$ for at least one b_i in the sample. The second alternative will quite generally be an event of probability zero, so a small regularizing $\varepsilon > 0$ must be kept in order to 'see' this contributions (if it exists).

We shall refer to the two contributions to (38) or (40), as $\overline{\rho}_s(\lambda)$ and $\overline{\rho}_c(\lambda)$, with

$$\overline{\rho}_s(\lambda) \simeq \frac{1}{\mathcal{N}}\sum_{\substack{i=1\\a_i=0}}^{\mathcal{N}} \mathcal{L}_\varepsilon(b_i+\lambda), \qquad \overline{\rho}_c(\lambda) \simeq \frac{1}{\pi\mathcal{N}}\sum_{\substack{i=1\\a_i>0}}^{\mathcal{N}} \frac{a_i+\varepsilon}{(a_i+\varepsilon)^2+(b_i+\lambda)^2}. \quad (41)$$

The population-dynamics algorithm itself is run with a small regularizing $\varepsilon > 0$ (as required in (2) to guarantee existence of the integral). While running the algorithm, we use $\varepsilon = 10^{-300}$, which is close to the smallest representable real number in double-precision arithmetic on the machines used for the numerics in order to minimize distorting effects due to this regularization.

We note, however, that when evaluating (41), the number of samples effectively contributing to $\overline{\rho}_s(\lambda)$—those with b_i in the interval $(-\lambda-\varepsilon, -\lambda+\varepsilon)$—is expected to scale as $\mathcal{N}P_0(-\lambda)\varepsilon$, and the fluctuations of this number, scaling as $\mathcal{O}(\sqrt{\mathcal{N}P_0(-\lambda)\varepsilon})$, will be much larger than the mean in the limit $\varepsilon \to 0$. We shall see this effect when naively evaluating the $\varepsilon \to 0$ limit for $P_0(-\lambda) \neq 0$ below. A reliable estimate of a regularized (smoothed) $P_0(-\lambda)$ requires to choose ε and $\mathcal{N}$ large enough to ensure $\mathcal{N}P_0(-\lambda)\varepsilon \gg 1$.

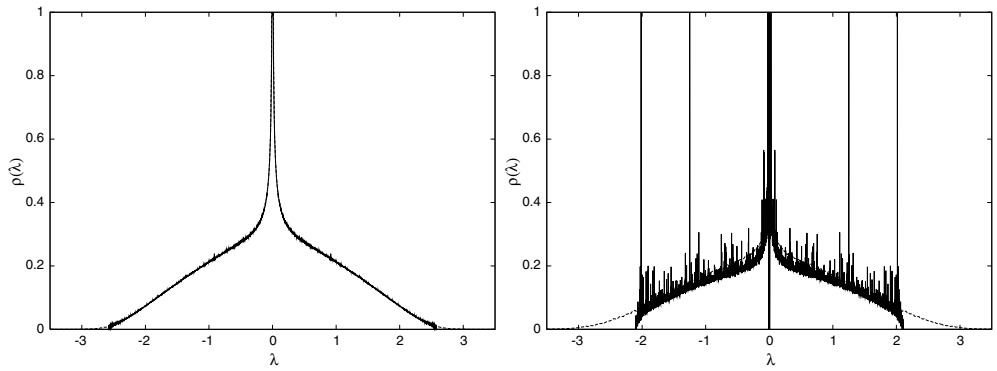

Figure 1. Spectral density for matrices defined on Poissonian random graphs with $c = 4$ (the left panel) and $c = 2$ (the right panel), having Gaussian random couplings with $\langle K_{ij}^2 \rangle = 1/c$. Full line: results obtained from the present theory; dashed line: results obtained from a sample of 2000×2000 matrices. In both cases $\varepsilon = 10^{-300}$ was used in the evaluation of (40).

3.1. Poisson random graphs—Gaussian couplings

Our first results pertain to sparse matrices defined on Poisson random graphs, with Gaussian couplings. The left panel of figure 1 shows spectral densities for the case of mean connectivity $c = 4$, having Gaussian random couplings with $\langle K_{ij}^2 \rangle = 1/c$. For this system we find an integrable power-law divergence of the form

$$\overline{\rho}(\lambda) \simeq 0.05|\lambda|^{-0.61}, \qquad \lambda \to 0, \tag{42}$$

and a δ peak at $\lambda = 0$, the latter originating from isolated sites in the ensemble. Results of numerical diagonalizations (using a sample of 500 $N \times N$ matrices with $N = 2000$ are shown for comparison, and the agreement is excellent.

The behaviour changes rather drastically if the average connectivity is reduced to $c = 2$—a value closer to the percolation threshold $c_c = 1$. In this case the spectral density shows strong fluctuations when naively evaluated with the same small regularizer. These fluctuations are not unexpected in view of our discussion at the beginning of this section; they originate from $\overline{\rho}_s$ in (41), and are related to the point spectrum associated with localized eigenstates coming from a collection of isolated finite clusters of all sizes in the ensemble. These exist for $c = 4$ as well, but their contribution is too small to be easily notable when combined with $\overline{\rho}_c$ in (40). In addition, there is a central δ peak as in the $c = 4$-case, which appears to be separated from the main bands by a gap; see the second panel in figure 2. The agreement with results of numerical diagonalization is fairly poor as it stands; in particular, exponential tails of localized states extending beyond the apparent edge of the central band are missed in this way. However, when (40) is evaluated with a regularizing $\varepsilon = 10^{-3}$ comparable to the resolution of the λ-scan, the agreement is once more excellent as shown in figure 2. It is worth noting in this context that numerical simulations, in which binning of eigenvalues is used to determine the spectral density *also imply a form of regularization*, and they do not distinguish continuous and singular contributions to the DOS if the distribution of the singular contribution $\overline{\rho}_s(\lambda)$ does not vary strongly on the scale of the binning resolution.

When displayed on a logarithmic scale, the results clearly reveal two interesting features: (i) a localization transition at $\lambda_c \simeq 2.295$, characterized by a vanishing continuous contribution $\overline{\rho}_c$ to (40) for $|\lambda| > \lambda_c$, and (ii) exponential (Lifshitz) tails [19] in the spectral density, related to localized states represented by the singular contribution $\overline{\rho}_s$ to (40)), and exhibited only

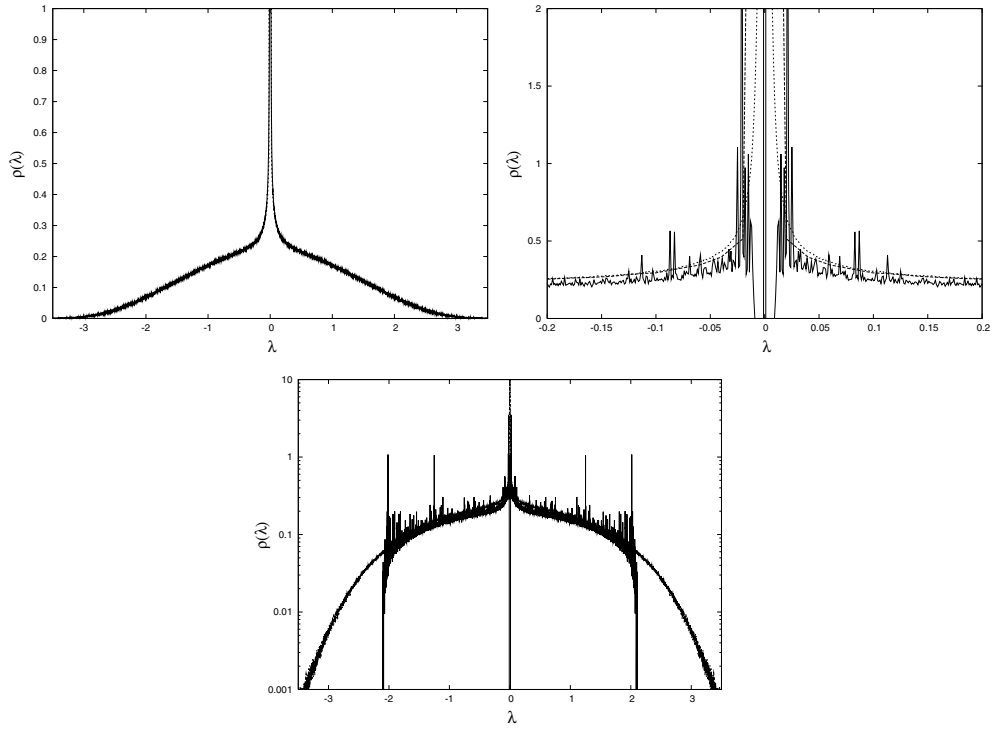

Figure 2. Upper left panel: spectral density for matrices defined on Poissonian random graphs with $c = 2$ as in the previous figure, but now evaluated with a regularizing $\varepsilon = 10^{-3}$ in (40) (full line). At the resolution given, the result is indistinguishable from the numerical simulation results (dashed line). Upper right panel: zoom into the central region comparing results obtained with the small regularizer, exhibiting a gap around the central peak (full line), with a larger regularizer $\varepsilon = 10^{-3}$ (short dashed line) and with results of numerical diagonalization (long dashed line). The same comparison is made in the lower panel for a larger portion of the spectrum on a logarithmic scale. The regularized $\varepsilon = 10^{-3}$ results are on this scale indistinguishable from those of the numerical simulations. Note the localization transition and the Lifshitz tails as discussed in the main text.

through regularization. We shall substantiate this analysis in the following subsection by looking at the behaviour inverse participation ratios. The same phenomena are seen for $c = 4$, where $\lambda_c \simeq 2.581$.

3.2. Inverse participation ratios and localization

In order to substantiate our identification of singular and continuous contributions to the spectral densities we look at inverse participation ratios (IPRs) of eigenstates as obtained from numerical diagonalizations. Given eigenvectors $\boldsymbol{v}$ of a (random) matrix, their IPRs are defined as

$$\mathrm{IPR}(\boldsymbol{v}) = \frac{\sum_{i=1}^{N} v_i^4}{\left(\sum_{i=1}^{N} v_i^2\right)^2}. \tag{43}$$

As eigenvectors can always be chosen to be normalized, we see that IPRs remain of order 1 for localized states which have a few $\mathcal{O}(1)$ eigenvector components—the extreme case being $\mathrm{IPR}(\boldsymbol{v}) = 1$ for $v_i = \delta_{i,i_0}$—whereas they are $\mathcal{O}(N^{-1})$ for fully extended states for which $v_i = \mathcal{O}(N^{-1/2})$ for all i.

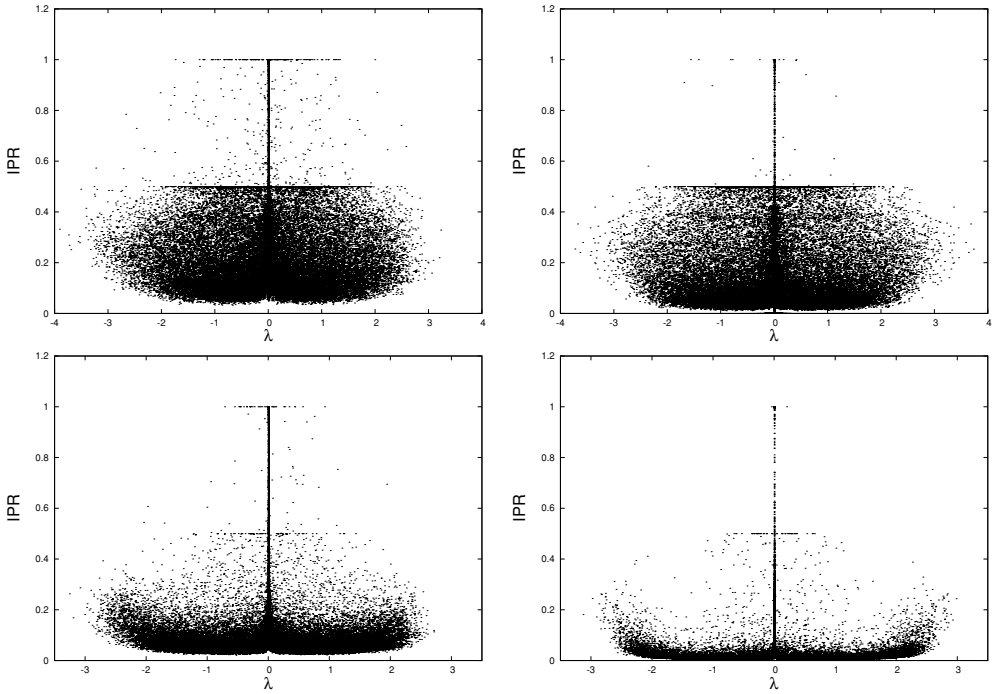

Figure 3. Scatter plots showing eigenvalue against IPRs for Poissonian random graphs with $c = 2$ (first row) and $c = 4$ (second row). The graphs in the left column correspond to $N = 100$, those in the right column to $N = 1000$.

Here we only produce a qualitative comparison for the two cases studied in the previous subsection, comparing IPRs computed for systems of size $N = 100$ and $N = 1000$, and using scatter plots of IPRs versus eigenvalues to exhibit the salient features. For similar results obtained earlier we refer to [21, 42]. As is clearly visible in figure 3, there remains a substantial fraction of states at all λ in the $c = 2$ case, which do *not* exhibit the N^{-1} scaling of IPRs expected for delocalized states; the tails, and a small central band in particular appear to be *dominated* by localized states. By contrast in the $c = 4$ case there is a notable depletion of states with $\mathcal{O}(1)$ IPRs, except for $\lambda = 0$ and in the tails of the spectrum. These findings are entirely consistent with our identifications made in the previous subsection.

Another test we have performed (not shown) is looking at the spectral density of *regular* random graphs with $c = 2$ and Gaussian couplings. Such graphs consist of an ensemble of closed linear chains of diverging length in the thermodynamic limit. Evaluating the spectral density for this system with the small regularizer, we *only* 'see' a δ peak at $\lambda = 0$, but once more also a band of localized states for a range of non-zero λ when evaluated with a larger ε—in perfect agreement with numerical diagonalization and with early results of Mott and Twose [43], according to which *all* states will be localized in disordered linear chains.

We note that the role of regularization in identifying localized states has been pointed out before using heuristics related to the evaluation of *local* densities of state [22].

We shall return to this issue in greater quantitative detail in a separate paper devoted to Anderson localization in discrete random Schrödinger operators defined on sparse random graphs [36].

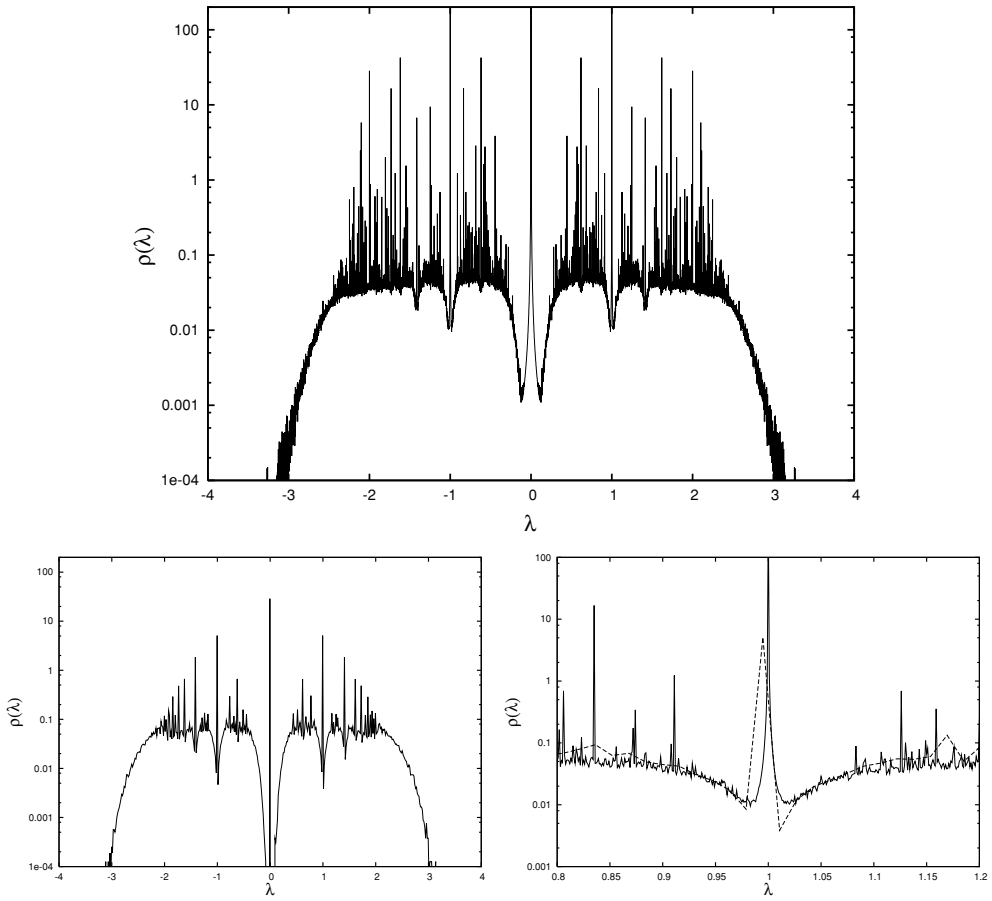

Figure 4. Comparison of spectral density for $K_{ij} = \pm 1/\sqrt{c}$, on a Poissonian random graph with $c = 1$ as computed via the present algorithm (main panel) with results from numerical diagonalization of $N \times N$ matrices of the same type with $N = 2000$ (lower left) and a direct comparison in the region around $\lambda = 1$.

3.3. Poisson random graphs—bimodal couplings

We can also look at coupling distributions different from Gaussian for the non-zero couplings, e.g. fixed $K_{ij} = 1/\sqrt{c}$ or bimodal $K_{ij} = \pm 1/\sqrt{c}$. As noted before [14], both give rise to the same spectral densities on large sparse (tree-like) graphs due to the absence of frustrated loops. It can also be seen as a consequence of the appearance of K^2 in (29).

We choose a Poissonian random graph *at* the percolation threshold $c = 1$ as an example that allows us to highlight both the strengths and the limitations of the present approach. It is known that all states will be localized for this system. This, too, is confirmed by evaluating the spectral density with the small regularizer.

In figure 4 we compare results of a λ-scan with resolution $\delta\lambda = 10^{-3}$, using a regularizer $\varepsilon = 10^{-4}$ for the scan. The smaller panels exhibit numerical diagonalization results, as well as a comparison between the two using a zoom into the region around $\lambda = 1$.

On the side of the strengths, we note that the spectral density obtained from our algorithm is able to display more details than can be exposed by simulation results obtainable at reasonable

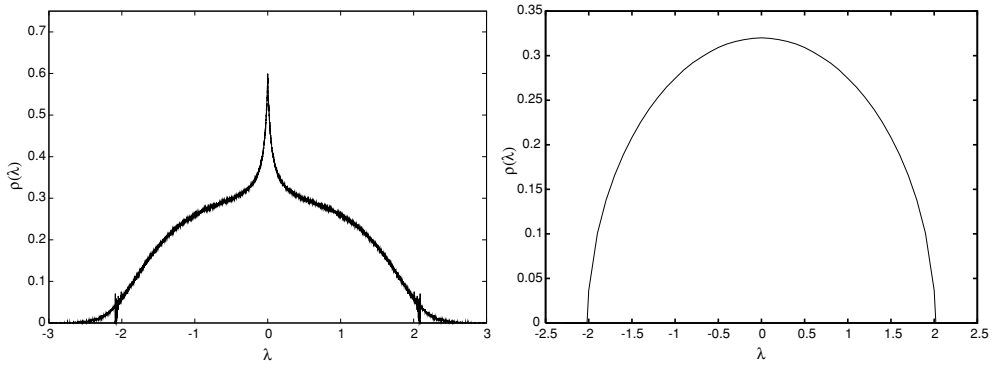

Figure 5. Spectral densities for a random graph with fixed connectivity $c = 4$ (left), and on a random graph with fixed non-random connectivity $c = 100$ (right).

effort. On the downside, one might note that the results for this system attain the status of semi-quantitative results, as they do depend on the chosen regularization, though in fairness it should be said that the same applies to the results obtained via numerical diagonalization where results vary with the binning resolution. In the present case this is due to the fact that the spectrum for most parts consists of a dense collection of δ peaks [44]. A notable deficiency is the broadening of δ peaks into Lorentzians of finite width, which creates artefacts around isolated δ peaks, exemplified here by the peak at $\lambda = 0$. Since the origin of this deficiency is understood, more precise details can, if desired, be recovered by choosing a smaller regularizing ε.

3.4. Regular and scale-free random graphs

In the present section we consider matrices defined on regular and scale-free random graphs.

3.4.1. Regular random graphs. Our theory applies unmodified to matrices defined on graphs with degree distributions other than Poissonian, as long as the *mean connectivity remains finite*. We use this fact to obtain spectra of matrices with Gaussian random couplings defined on regular random graphs with fixed connectivity c, choosing $\langle K_{ij}^2 \rangle = 1/c$ for the couplings. Results for $c = 4$ and $c = 100$ are shown in figure 5. The $c = 4$ results are in perfect agreement with simulations; results are analogous to previous cases, including the presence of a localization transition at $\lambda_c \simeq 2.14$.

The second example is chosen as a *test* to see whether the present algorithm exhibits the correct limiting behaviour in the large c limit where Wigner's semi-circular law [25] should be recovered [14]. This limit can also be extracted from the fixed point equations. It is somewhat easier to verify for the equations pertaining to single instances [35] than for the ensemble.

As yet another test (not shown), we note that results we obtain for regular random graphs with constant weights $K_{ij} \equiv 1$ are in perfect agreement with exact results of McKay [45].[2]

[2] I am indebted to John Keating for pointing out this reference to me.

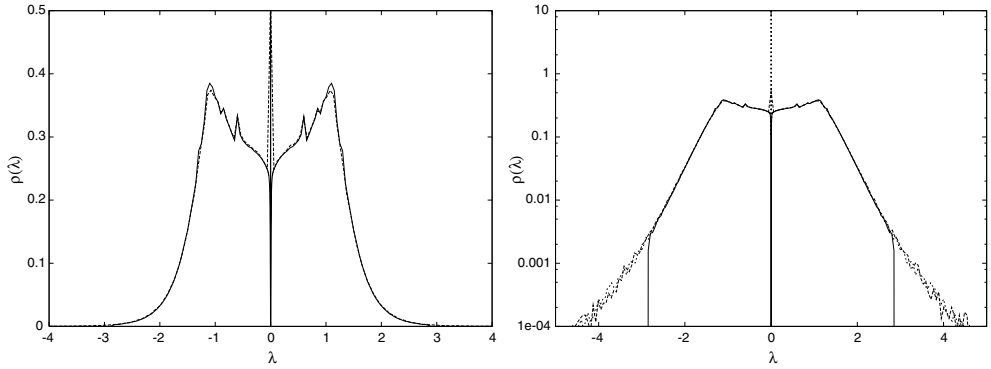

Figure 6. Spectral density for $K_{ij} = \pm 1/\sqrt{c}$ on a random graph with power-law degree distribution of average connectivity $c \simeq 2.623$. Left panel: results obtained with small regularizer (full line), and numerical diagonalization results from a sample of 500 matrices of dimension $N = 2000$ (dashed line). Right panel: the same results displayed on a logarithmic scale, this time with results regularized at $\varepsilon = 10^{-3}$ (short dashed line) included.

3.4.2. Scale-free graphs. We have also looked at a scale-free graph with connectivity distribution given by $p(k) = P_0 k^{-\gamma}$ with $\gamma = 4$ and a lower cut-off at $k = 2$. Results shown in figure 6 reveal a continuous central band, and localized states for $|\lambda| > \lambda_c \simeq 2.85$ much as in the other cases. For the present system, the tails in the spectral density follow a power law of the form $\overline{\rho}(\lambda) \sim \lambda^{1-2\gamma}$ [17, 46].

Comparison with exact diagonalization results is facilitated by a fast algorithm that allows us to generate sparse graphs with arbitrary degree distribution [47].

3.5. Graph Laplacians

Let us finally look at matrices with row constraints, such as related to discrete graph Laplacians.

The discrete graph Laplacian of a graph with connectivity matrix $C = \{c_{ij}\}$ has matrix elements

$$\Delta_{ij} = c_{ij} - \delta_{ij} \sum_k c_{ik}. \tag{44}$$

A quadratic form involving the Laplacian can be written in the form

$$\frac{1}{2} \sum_{ij} \Delta_{ij} u_i u_j = -\frac{1}{4} \sum_{ij} c_{ij} (u_i - u_j)^2. \tag{45}$$

As before we shall be interested in more general matrices with zero row-sum constraint of the form

$$M_{ij} = c_{ij} K_{ij} - \delta_{ij} \sum_k c_{ik} K_{ik}. \tag{46}$$

To evaluate the spectral density within the present framework one would thus have to compute

$$\overline{Z_N^n} = \int \prod_{ia} \frac{\mathrm{d}u_{ia}}{\sqrt{2\pi/\mathrm{i}}} \exp\left\{ -\frac{\mathrm{i}}{2} \lambda_\varepsilon \sum_{i,a} u_{ia}^2 + \frac{c}{2N} \sum_{ij} \left(\left\langle \exp\left(\frac{\mathrm{i}K}{2} \sum_a (u_{ia} - u_{ja})^2 \right) \right\rangle_K - 1 \right) \right\}$$

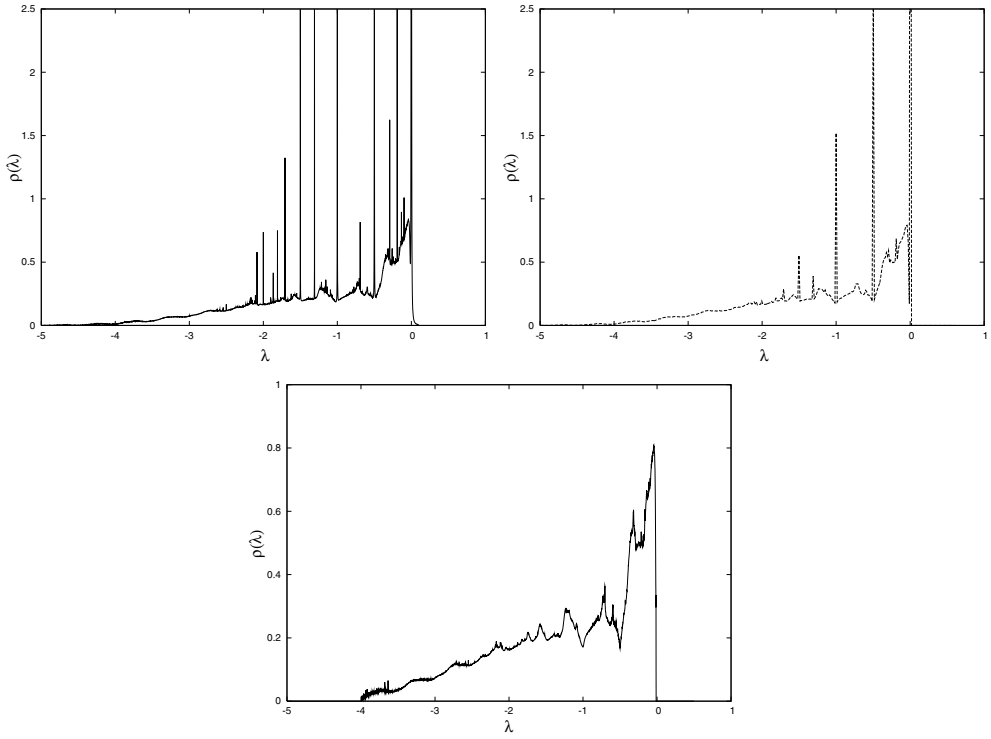

Figure 7. Spectral density for the Laplacian on a Poissonian random graph with $c = 2$ as computed via the present algorithm. Upper left panel: $\varepsilon = 10^{-3}$ results; upper right panel: results from numerical diagonalization of $N \times N$ matrices of the same type with $N = 2000$. Lower panel: continuous part of the spectrum obtained using $\varepsilon = 10^{-300}$ as a regularizer.

instead of (5). The required modification has, of course, been noted earlier [15, 48]. The resulting problem constitutes precisely (the harmonic variant of) the translationally invariant systems, for which the framework in [33] was developed in the first place. The general theory can be copied word by word, and the fixed point equations (31), (32) remain formally unaltered except for the change in $Z_2(\omega, \omega', K)$ in (24), owing to the modified interaction term, which gives rise to a modified expression for $\hat{\Omega}(\omega', K)$ in (29). We obtain

$$\hat{\Omega}(\omega', K) = \frac{K\omega'}{K - \mathrm{i}\omega'} \tag{47}$$

instead of (29). Figure 7 shows the spectrum of a Laplacian for a Posisson random graph with $c = 2$, comparing our solution (upper left panel) computed with $\varepsilon = 10^{-3}$ with numerical diagonalization results in the upper right panel. We use $K_{ij} \equiv 1/c$ for the non-zero matrix elements in this case. Results obtained with a small regularizer $\varepsilon = 10^{-300}$ exhibiting only the continuous part of the spectrum are shown in the lower panel.

As in the other cases, we observe localization transitions, here at $\lambda_c \simeq -3.98$, and another one at $\lambda_c \simeq -0.015$. Preliminary results are compatible with the suggestion that Lifshitz-type behaviour, established in [19] for the spectral density close to $\lambda = 0$ below the percolation threshold at $c < 1$, might persist for $c > 1$.

We note that an iterative solution of the Bray–Rodgers integral equation for this case [15], which appears to be effective in the small c limit, has been proposed and investigated in [18].

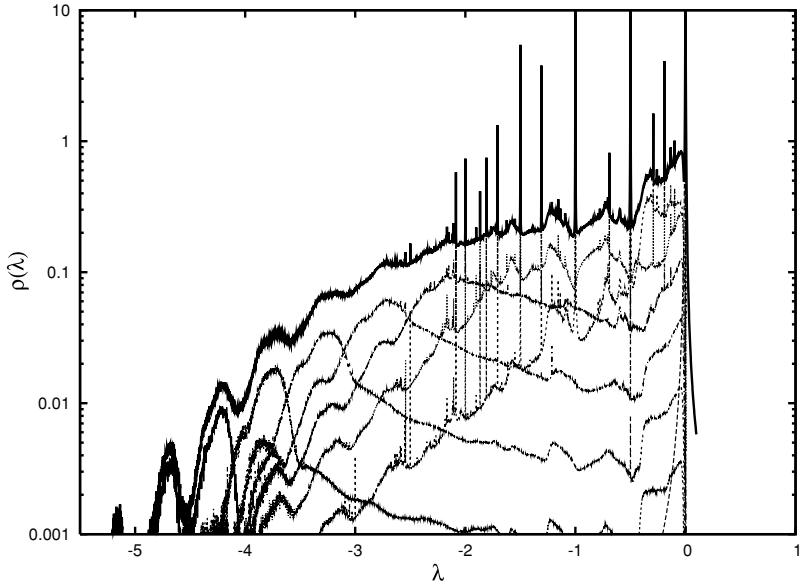

Figure 8. Spectral density for the Laplacian on a Poissonian random graph with $c = 2$ (full upper line), shown together with its unfolding according to contributions of different coordinations, as discussed in the main text.

3.6. Unfolding spectral densities

As a last item in this study we look at the possibility of unfolding the spectral density according to contributions of local densities of state, coming from vertices of different coordinations, as suggested by equation (33). This method has been used in [33] to look at distributions of Debye-Waller factors in amorphous systems, unfolded according to local coordinations. In the present context it may provide an interesting diagnostic tool to help understanding localization phenomena.

Figure 8 exhibits the spectrum of the graph Laplacian shown in the previous figure along with its unfolding into contributions of local densities of state with different coordinations.

The clearly identifiable humps in the figure correspond from left to right to $k = 9$, $k = 8$, $k = 7$, $k = 6$, $k = 5$, $k = 4$ and $k = 3$, which easily allows us to identify the corresponding contributions to the spectral density, the contribution of $k = 2$ gives rise to several notable humps in the spectral density, and together with the $k = 1$ contribution is mainly responsible for the dip at $\lambda = -1$. The $k = 0$ contribution is mainly responsible for the δ-peak at $\lambda = 0$ (which is broadened into a Lorentzian of width $\varepsilon = 10^{-3}$ due to the regularization, as discussed earlier.

The present example clearly shows that—somewhat paradoxically—the well-connected sites are those providing the dominant contributions to localized states in the lower band-edge Lifshitz tails with $\lambda < -3.98$. Conversely, the sites with small k appear to contribute mostly to the spectral density at *small* $|\lambda|$ and in particular to the localized states in this region at $\lambda > -0.015$. A similar observation has in fact been made before in [26].

4. Conclusions

In the present paper we have used a reformulation of the replica approach to the computation of spectral densities for sparse matrices, which allows us to obtain spectral densities in the

thermodynamic limit to any desired detail—limited only by computational resources. Our method is versatile in that it allows us to study systems with arbitrary degree distributions, as long as they give rise to connectivity distributions with finite mean. A cavity approach that emphasizes results on finite instances will appear elsewhere [35]. Although our version of the replica symmetric ansatz can, and has been made plausible in several ways, a rigorous proof of its correctness is still missing.

Several tests are available, though e.g., all our results are in excellent agreement with direct numerical diagonalization studies. We have checked that our ansatz reproduces the Wigner semi-circle law for the spectral density in the limit of large average coordination c as it should [14]. We also noted agreement between our results and available exact results for connectivity matrices of regular random graphs [45]. Large and small λ asymptotics remain to be investigated.

It is one of the surprising results of the present study that our method allows us to expose the separate contributions of localized and extended states to the spectral density, and thereby to study localization transitions. We have confirmed this identification qualitatively using IPRs, but also by looking at cases where states are *known* to be localized, such as Poisson random graphs at or below the percolation threshold, or random chains (here represented as regular random graphs with $c = 2$ and Gaussian couplings). We shall explore the issue of localization in greater quantitative detail in a separate publication. Indeed, with results for graph Laplacians in hand, the step towards a study of discrete random Schrödinger operators and Anderson localization in such systems is just around the corner [36]. There are indications that the localization transitions seen in the present approach are proper continuous phase transitions, accompanied e.g. by effects of critical slowing down in the population dynamics algorithm used to solve the self-consistency equations. Within our formulation, we have not been able to identify the symmetry that would be broken at these transitions. This issue clearly deserves further investigation, as does the issue of determining critical exponents governing the transitions.

As a drawback of our method we note that results in regions dominated by localized states do depend on the regularization chosen. The way in which they do is, however, understood (via the broadening of δ-peaks into Lorentzians of finite width) and can be taken into account if desired.

We believe our results to constitute an improvement over previous asymptotic results as well as over results obtained by closed form approximations. They may open the way to further interesting lines of research. Let us here mention just a few such examples: within RMT proper, one might wish to further investigate the degree of universality of level correlations in these systems [49]; one could refine the random matrix analysis of financial cross-correlations [7] by taking non-trivial degree distributions of economic interactions into account, or one might wish to look at finite connectivity variants of random reactance networks [50], taking e.g. regular connectivity 4 to compare with results of numerical simulations of such systems on two-dimensional square lattices.

A generalization to asymmetric matrices using both the cavity method and a replica approach for the ensemble along the lines of [51] is currently under investigation in our group [52]. Other problems we have started to look at are spectra of modular systems and small-world networks [53].

While we were revising the present paper, a preprint of G Bianconi appeared [54], in which some of our results were independently derived along similar lines.

Acknowledgments

It is a pleasure to thank Güler Ergün, Jort van Mourik, Isaac Pérez-Castillo, Tim Rogers and Koujin Takeda for illuminating discussions. Jort van Mourik also kindly supplied instances of scale free-random graphs to allow comparison of ensemble results and results from numerical diagonalization in this case.

Appendix. Population dynamics

The stochastic algorithm used to solve (31), (32) takes the following form. Populations $\{\omega_i; 1 \leqslant i \leqslant N_p\}$ and $\{\hat{\omega}_i; 1 \leqslant i \leqslant N_p\}$ are randomly initialized with $\mathrm{Re}\,\omega_i > 0$ and $\mathrm{Re}\,\hat{\omega}_i > 0$.

Then the following steps are iterated:

(1) Generate a random $k \sim \frac{k}{c} p_c(k)$.
(2) Randomly select $k-1$ elements from $\{\hat{\omega}_i; 1 \leqslant i \leqslant N_p\}$; compute

$$\Omega = \mathrm{i}\lambda_\varepsilon + \sum_{j=1}^{k-1} \hat{\omega}_{i_j}, \tag{A.1}$$

and replace ω_i by Ω for a randomly selected $i \in \{1, \ldots, N_p\}$.
(3) Select $j \in \{1, \ldots, N_p\}$ at random, generate a random K according to distribution of bond strengths; compute

$$\hat{\Omega} = \frac{K^2}{\omega_j} \qquad \left(\text{or } \hat{\Omega} = \frac{K\omega_j}{K - \mathrm{i}\omega_j} \text{ for zero row sums}\right), \tag{A.2}$$

and replace $\hat{\omega}_i$ by $\hat{\Omega}$ for a randomly selected $i \in \{1, \ldots, N_p\}$.
(4) Return to **(1)**.

This algorithm is iterated until populations with stable distributions of $\{\hat{\omega}_i; 1 \leqslant i \leqslant N_p\}$ and $\{\omega_i; 1 \leqslant i \leqslant N_p\}$ are attained.

A variant of this algorithm when implemented on instances of real graphs generates the belief propagation or cavity equations for this problem, as studied in [35]. It can be derived directly in terms iterative evaluations of (2) on locally tree-like graphs.

References

[1] Wigner E P 1951 On the statistical distribution of the widths and spacings of nuclear resonance levels *Proc. Cam. Phil. Soc.* **47** 790–8
[2] May R M 1972 Will a large complex system be stable? *Nature* **238** 413–4
[3] Thouless D J 1977 Maximum metallic resistance in thin wires *Phys. Rev. Lett.* **39** 1167–9
[4] Bohigas O, Giannoni M J and Schmit C 1984 Characterization of chaotic quantum spectra and universality of level fluctuation laws *Phys. Rev. Lett.* **52** 1–4 (DOI:D10.1103/PhysRevLett.52.1)
[5] Verbaarschot J 1994 The spectrum of the QCD dirac operator and chiral random matrix theory: the threefold way *Phys. Rev. Lett.* **72** 2531–3
[6] Laloux L, Cizeau P, Bouchaud J-P and Potters M 1999 Noise dressing of financial correlation matrices *Phys. Rev. Lett.* **83** 1467–70
[7] Plerou V, Gopikrishnan P, Rosenow B, Amaral L A N and Stanley H E 1999 Universal and non-universal properties of cross-correlations in financial time series *Phys. Rev. Lett.* **83** 1471–4
[8] Cavagna A, Giardina I and Parisi G 1999 Analytic computation of the instantaneous normal modes spectrum in low density liquids *Phys. Rev. Lett.* **83** 108–11
[9] Broderix K, Bhattacharya K K, Cavagna A, Zippelius A and Giardina I 2001 Saddles on the potential energy landscape of a Lennard–Jones liquid *AIP Conf. Proc.* **553** 23–7

[10] Kühn R and Horstmann U 1997 Random matrix approach to glassy physics: low temperatures and beyond *Phys. Rev. Lett.* **78** 4067–70
[11] Kühn R 2003 Universality in glassy low-temperature physics *Europhys. Lett.* **62** 313–9
[12] Keating J P and Snaith N C 2000 Random matrix theory and L-functions at $s = 1/2$ *Commun. Math. Phys.* **214** 91–110
[13] Guhr T, Müller-Groeling A and Weidenmüller H A 1998 Random matrix theories in quantum physics: common concepts *Phys. Rep.* **299** 190–425
[14] Rodgers G J and Bray A J 1988 Density of states of a sparse random matrix *Phys. Rev.* B **37** 3557–62
[15] Bray A J and Rodgers G J 1988 Diffusion in a sparsely connected space: a model for glassy relaxation *Phys. Rev.* B **38** 11461–70
[16] Albert R and Barabási A-L 2002 Statistical mechanics of complex networks *Rev. Mod. Phys.* **74** 47–97
[17] Dorogovtsev S N, Goltsev A V, Mendes J F F and Samukhin A N 2003 Spectra of complex networks *Phys. Rev.* E **68** 046109
[18] Broderix K, Aspelmeyer T, Hartmann A K and Zippelius A 2001 Stress relaxation of near-critical gels *Phys. Rev.* E **64** 021404
[19] Khorunzhiy O, Kirsch W and Müller P 2006 Lifshitz tails for spectra of Erdös–Renyi random graphs *Ann. Appl. Prob.* **16** 295–309 (*Preprint* math-ph/0502054)
[20] Griffiths R B 1969 Nonanalytic behavior above the critical point in a random Ising ferromagnet *Phys. Rev. Lett.* **23** 17–9
[21] Evangelou S N and Economou E N 1992 Spectral density singularities, level statistics and localization in a sparse random matrix ensemble *Phys. Rev. Lett.* **68** 361–4
[22] Ciliberti S, Grigera T S, Martín-Mayor V, Parisi G and Verrocchio P 2005 Anderson localization in Euclidean random matrices *Phys. Rev.* B **71** 153104
[23] Fyodorov Y V and Mirlin A D 1991 On the density of states of sparse random matrices *J. Phys. A: Math. Gen.* **24** 2219–23
[24] Khorunzhy O, Shcherbiba M and Vengerovsky V 2004 Eigebvalue distribution of large weighted random graphs *J. Math. Phys.* **45** 1648–72
[25] Wigner E P 1958 On the distribution of the roots of certain symmetric matrices *Ann. Math.* **67** 325–7
[26] Biroli G and Monasson R 1999 A single defect approximation for localized states on random lattices *J. Phys. A: Math. Gen.* **32** L255–61
[27] Semerjian G and Cugliandolo L F 2002 Sparse random matrices: the eigenvalue spectrum revisited *J. Phys. A: Math. Gen.* **35** 4837–51
[28] Nagao T and Rodgers G J 2008 Spectral density of complex networks with a finite mean degree *Preprint* arXiv:cond-mat/08031042
[29] Goh K-I, Kahng B and Kim D 2001 Spectra and eigenvectors of scale-free networks *Phys. Rev.* E **64** 051903
[30] Monasson R 1998 Optimization problems and replica symmetry breaking in finite connectivity spin-glasses *J. Phys. A: Math. Gen.* **31** 513–29
[31] Mézard M and Parisi G 2001 The Bethe lattice spin glass revisited *Eur. Phys. J.* B **20** 217–33 (DOI:10.1007/PL00011099)
[32] Coolen A C C, Skantzos N S, Pérez-Castillo I, Pérez-Vicente C J, Hatchett J P L, Wemmenhove B and Nikoletopoulos T 2005 Finitely connected vector spin systems with random matrix interactions *J. Phys. A: Math. Gen.* **38** 8289–317
[33] Kühn R, van Mourik J, Weigt M and Zippelius A 2007 Finitely coordinated models for low-temperature phases of amorphous systems *J. Phys. A: Math. Theor.* **40** 9227–52
[34] Edwards S F and Jones R C 1976 The eigenvalue spectrum of a large symmetric random matrix *J. Phys. A: Math. Gen.* **9** 1595–603
[35] Rogers T, Pérez-Castillo I, Kühn R and Takeda K 2008 Cavity approach to the spectral density of sparse symmetric random matrices *Preprint* arXiv:0803.1553
[36] Kühn R and van Mourik J 2008 Localization in random-Schrödinger operators on sparse random graphs in preparation
[37] Rodgers G J, Austin K, Kahng B and Kim D 2005 Eigenvalue spectra of complex networks *J. Phys. A: Math. Gen.* **38** 9431–7
[38] Kim D and Kahng B Spectral densities of scale-free networks *Preprint* arXiv:cond-mat/0703055
[39] Viana L and Bray A J 1985 Phase diagrams for dilute spin glasses *J. Phys. C: Solid State Phys.* **18** 3037–51
[40] Kanter I and Sompolinsky H 1987 Mean-field theory of spin-glasses with finite ccoordination number *Phys. Rev. Lett.* **58** 164–7
[41] Goldbart P M, Castillo H M and Zippelius A 1996 Randomly crosslinked macromolecular systems: vulcanisation transition to and properties of the amorphous solid state *Adv. Phys.* **45** 393–468

[42] Evangelou S N 1992 A numerical study of sparse random matrices *J. Stat. Phys.* **69** 361–83
[43] Mott N F and Twose W D 1961 The theory of impurity conduction *Adv. Phys.* **10** 107–63
[44] Golinelli O 2003 Statistics of delta peaks in the spectral density of large random trees *Preprint* arXiv:cond-mat/0301437
[45] McKay B D 1981 The expected eigenvalue distribution of a large regular graph *Linear Algebr. Appl.* **40** 203–16
[46] Mihail M and Papadimitriou C 2002 On the eigenvalue power law *Lect. Notes Comput. Sci.* **2483** 254–62 (DOI:10.1007/3-540-45726-7_20)
[47] van Mourik J and Kabashima Y 2003 The polynomial error probability for LDPC codes *Preprint* arXiv:cond-mat/0310177
[48] Stäring J, Mehlig B, Fyodorov Y V and Luck J M 2003 Random symmetric matrices with a constraint: the spectral density of random impedance networks *Phys. Rev.* E **67** 047101
[49] Mirlin A D and Fyodorov Y V 1991 Universality of level correlation function of sparse random matrices *J. Phys. A: Math. Gen.* **24** 2273–86
[50] Fyodorov Y V 1999 Spectral properties of random reactance networks and random matrix pencils *J. Phys. A: Math. Gen.* **32** 7429–46
[51] Haake F, Izrailev F, Lehmann N, Saher D and Sommers H-J 1992 Statistics of complex levels of random matrices for decaying systems *Z. Phys.* B **88** 359–70
[52] Anand K and Rogers T 2008 in preparation
[53] Ergün G and Kühn R 2008 Spectra of sparsely connected modular random matrices in preparation
[54] Bianconi G 2008 Spectral properties of complex networks *Preprint* arXiv:cond-mat/080417444